Organometallics versus P_4 Complexes of Group 11 Cations: Periodic Trends and Relativistic Effects in the Involvement of (n−1)d, ns, and np Orbitals in Metal−Ligand Interactions

Hui-Chung Tai,[†] Ingo Krossing,[‡] Michael Seth,[§] and Dirk V. Deubel*[,∥,⊥]

Academia Sinica, Taipei, Taiwan 11529, Republic of China, Department of Chemistry, University of Karlsruhe, 76128 Karlsruhe, Germany, Department of Chemistry, University of Calgary, Canada T2N 1N4, Swiss Center for Scientific Computing, ETH Zürich, 6928 Manno, Switzerland, and Department of Chemistry and Applied Biosciences, Computational Science Laboratory, ETH Zürich, 6900 Lugano, Switzerland

Received October 20, 2003

The nature of the bonding in ethylene and η^2-P_4 complexes, $M(C_2H_4)_2^+$ and $M(\eta^2\text{-}P_4)_2^+$, of group 11 metal cations (M = Cu, Ag, Au) has been explored by density functional calculations. On the basis of the evaluation of symmetry orbitals, the contributions from the interactions of ligand orbitals with metal ns, np, and (n−1)d orbitals have been investigated. The analysis shows that the metal−ligand bonds in the organometallics and phosphorus complexes fit to a unified scheme, whereas traditional concepts such as the isolobality principle would hardly predict such a bonding analogy between C_2H_4 and P_4 complexes. Bond energies increasing in the order Ag < Cu < Au have been predicted. The stronger metal−ligand bonds in the gold(I) compounds compared to those in the silver(I) compounds can be elucidated by the relativistic stabilization of the orbital interactions, particularly of those involving 6s and 5d orbitals. The stronger metal−ligand bonds in $Cu(\eta^2\text{-}P_4)_2^+$ compared to those in the experimentally known $Ag(\eta^2\text{-}P_4)_2^+$ can be attributed partly to the strong back-donation from metal 3d orbitals to vacant ligand orbitals. This result stands in sharp contrast to the common belief that first-row transition metals form weaker bonds to ligands than do their second-row analogues because of a comparably small overlap between ligand orbitals and metal 3d orbitals.

Downloaded by NAT LIB UKRAINE on July 5, 2009
Published on April 15, 2004 on http://pubs.acs.org | doi: 10.1021/om034246z

Introduction

$Ag(\eta^2\text{-}P_4)_2^+$, the first homoleptic metal-phosphorus cation, was recently synthesized by one of us.[1] The synthesis succeeded due to the presence of weakly coordinating counterions,[2] a concept that enables the development of new catalytic systems and the design of fascinating species.[3] Understanding the bonding in these novel compounds is a major challenge. An analysis of electron density[4] in $Ag(\eta^2\text{-}P_4)_2^+$ and in the ethylene complex $Ag(C_2H_4)^+$ suggests fundamentally different interactions in the two species.[5] Traditional concepts such as the isolobality principle would also hardly predict a similar bonding in the two silver species.[6] In contrast, we recently gained a unified view of the bonding situation in the two complexes and showed that the interactions in organometallics and phosphorus complexes are essentially identical.[7] This conclusion was based on an analysis[8,9] of the energy contributions from symmetry orbitals to the orbital interactions. Our study[7] is a new chapter in the success story of orbital symmetry in chemistry, which was pioneered by Woodward and Hoffmann's work.[10] High molecular symmetry is also useful in the understanding of phosphorus analogues of ferrocene. Frenking and co-workers[11] recently compared the bonding in ferrocene and decaphosphaferrocene. An experimental highlight is the synthesis of

* Corresponding author. E-mail: metals-in-medicine@phys.chem.ethz.ch.
[†] Academia Sinica.
[‡] University of Karlsruhe.
[§] University of Calgary.
[∥] Swiss Center for Scientific Computing.
[⊥] Computational Science Laboratory, ETH Zürich.

(1) Krossing, I. *J. Am. Chem. Soc.* **2001**, *123*, 4603.
(2) Krossing, I. *Chem. Eur. J.* **2001**, *7*, 490.
(3) (a) Krossing, I.; Raabe, I. *Angew. Chem., Int. Ed.* **2001**, *40*, 4406. (b) Cameron, T. S.; Decken, A.; Dionne, I.; Fang, M.; Krossing, I.; Passmore, J. *Chem. Eur. J.* **2002**, *8*, 3368. (c) Gonsior, M.; Krossing, I.; Müller L.; Raabe, I.; Jansen, M.; van Wüllen, L. *Chem. Eur. J.* **2002**, *8*, 4479. (d) Krossing, I. *J. Chem. Soc. Dalton* **2002**, 500. (e) Adolf, A.; Gonsior, M.; Krossing, I. *J. Am. Chem. Soc.* **2002**, *124*, 7111. (f) Krossing, I.; Bihlmeier, A.; Raabe, I.; Trapp, N. *Angew. Chem., Int. Ed.* **2003**, *42*, 1531. (g) Krossing, I.; Reisinger, A. *Angew. Chem., Int. Ed.* **2003**, *42*, 5725.
(4) Bader, R. F. W. *Atoms in Molecules*; Clarendon Press: Oxford, England, 1994.
(5) Krossing, I.; van Wüllen, L. *Chem. Eur. J.* **2002**, *8*, 700.
(6) Hoffmann, R. *Angew. Chem., Int. Ed. Engl.* **1982**, *21*, 711.
(7) Deubel, D. V. *J. Am. Chem. Soc.* **2002**, *124*, 12312.
(8) Pioneering work: (a) Morokuma, K. *J. Chem. Phys.* **1971**, *55*, 1236. (b) Ziegler, T.; Rauk, A. *Theor. Chim. Acta* **1977**, *46*, 1.
(9) Reviews: (a) Bickelhaupt, F. M.; Baerends, E. J. In *Reviews in Computational Chemistry*; Lipkowitz, K. B.; Boyd, D. B., Eds.; Wiley-VCH: New York, 2000; Vol. 15, p 1. (b) Frenking, G.; Fröhlich, N. *Chem. Rev.* **2000**, *100*, 717. (c) Frenking, G.; Wichmann, K.; Fröhlich, N.; Loschen, C.; Lein, M.; Frunzke, J.; Rayón, V. M. *Coord. Chem. Rev.* **2003**, *238*, 55.
(10) Woodward, R. B.; Hoffmann, R. *The Conservation of Orbital Symmetry*; Weinheim: VCH, 1970.
(11) (a) Lein, M.; Frunzke, J.; Timoshkin, A.; Frenking, G. *Chem. Eur. J.* **2001**, *7*, 4155. (b) Frunzke, J.; Lein, M.; Frenking, G. *Organometallics* **2002**, *124*, 3351.

10.1021/om034246z CCC: $27.50 © 2004 American Chemical Society
Publication on Web 04/15/2004

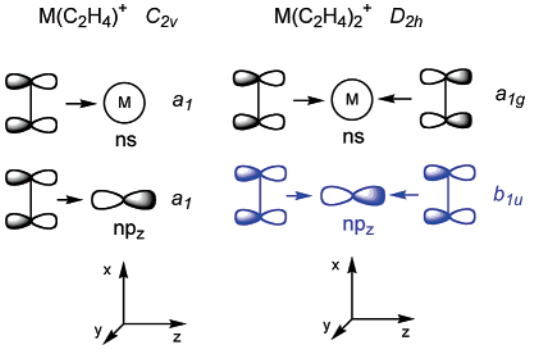

Figure 1. Selected symmetry orbitals in monoethylene complexes (C_{2v} symmetry) and diethylene complexes (D_{2h} symmetry). σ donation from the ethylene HOMO into vacant *n*s and *n*p orbitals.

$Ti(\eta^5\text{-}P_5)_2^{2-}$ by Urnezius et al.,[12,13] a sandwich with "inorganic bread".

The objective of this study is to gain a better understanding of the bonding in metal complexes, focusing on the importance of the metal *n*s, *n*p, and (*n*−1)d orbitals in metal−ligand interactions. In particular, we aim to explore how relativistic effects influence the periodic trends in orbital interactions. Both ethylene and phosphorus species of coinage-metal cations have been investigated because of a historical and current interest in these compounds.[14]

The bonding in organometallics of group 11 cations has fascinated chemists longer than two decades. Ziegler and Rauk[15] reported a pioneering study of the ethylene complexes. Hertwig et al.[16] presented a more recent piece of work and looked into the contributions from relativistic effects. However, these former studies considered only the $M(C_2H_4)^+$ complexes, which are C_{2v}-symmetric. As the C_{2v} point group does not contain a symmetry center, the contributions from metal s, p, and d orbital interactions to the bond energy are not accessible. Therefore, insight was limited to the importance of σ and π interactions. Figure 1 demonstrates this consideration in the case of σ donation from the ethylene HOMO into vacant *n*s and *n*p orbitals of the metal. The energy contributions from these two interactions in the C_{2v}-symmetric $Ag(C_2H_4)^+$ structure cannot be resolved, because both interactions belong to a_1 orbital symmetry. In contrast, the analysis of the D_{2h}-symmetric structure of $Ag(C_2H_4)_2^+$ assigns the metal s orbital to a_{1g} and the metal p_z orbital to b_{1u}. Hence, the energy contributions of each orbital type become accessible.

Molecular Geometries and Bond Energies

In this section, we report the calculated structures and energies of the ML_2^+ complexes (M = Cu, Ag, Au; L = P_4, C_2H_4). Table 1 shows theoretically predicted molecular structures of $M(P_4)_2^+$ and $M(C_2H_4)_2^+$ calculated using gradient-corrected density functional theory (DFT) at the BLYP level[17,18] and very large basis sets within the nonrelativistic (NR) and relativistic (R) approaches,[19] as implemented in the Amsterdam Density Functional program package (ADF).[20] Figure 2 displays the NR and R structures of the gold complexes. Structures calculated at the B3PW91 level using a relativistic effective core potential[21] are also presented in Table 1 for comparison. Since the D_{2h}- and D_{2d}-symmetric isomers are found to have the same energy, we will focus in the discussion on the D_{2h} isomers.[22] The computed structures of $Ag(P_4)_2^+$ are in good agreement with experimental structures;[1,7] the consideration of exact exchange improves the calculated bond distances between the metal-bound phosphorus atoms.

The calculations show that the Au−P bonds (NR: 2.74 Å, R: 2.50 Å) contract strongly due to relativity and become shorter than the Ag−P bonds (NR: 2.66 Å, R: 2.57 Å). Relativistic metal−ligand bond contractions are well documented and arise from the reduction of kinetic energy.[23] As a secondary effect, we observe that the P−P bond between the metal-bound phosphorus atoms is elongated due to relativity; for instance, the P1−P2 distance in the gold complexes is predicted to increase from 2.37 Å (NR) to 2.45 Å (R). The same tendency of the interatomic distances holds for the ethylene com-

Downloaded by NAT LIB UKRAINE on July 5, 2009
Published on April 15, 2004 on http://pubs.acs.org | doi: 10.1021/om034246z

(12) Urnezius, E.; Brennessel, W. W.; Cramer, C. J.; Ellis, J. E.; Schleyer, P. V. *Science* **2002**, *295*, 832.
(13) (a) Sitzmann, H. *Angew. Chem., Int. Ed.* **2002**, *41*, 2723. (b) Mathey, F. *Angew. Chem., Int. Ed.* **2003**, *42*, 1578.
(14) (a) Basch, H. *J. Chem. Phys.* **1972**, *56*, 441. (b) Merchan, M.; Gonzalez-Luique, R.; Nebot-Gil, I.; Tomas, F. *Chem. Phys. Lett.* **1985**, *112*, 412. (c) Fisher, E. R.; Armentrout, P. B. *J. Phys. Chem.* **1990**, *94*, 4251. (d) Hill, Y. D.; Freiser, B. S.; Bauschlicher, C. W. *J. Am. Chem. Soc.***1991**, *113*, 1507. (e) Guo, B. C.; Castleman, A. W. *Chem. Phys. Lett.* **1991**, *181*, 16. (f) Sodupe, M.; Bauschlicher, C. W.; Langhoff S. R.; Partridge, H. *J. Phys. Chem.* **1992**, *96*, 2118. (g) Hrusák, J.; Hertwig, R. H.; Schröder, D.; Schwerdtfeger, P.; Koch, W.; Schwarz, H. *Organometallics* **1995**, *14*, 1284. (h) Hertwig, R. H.; Hrusák, J.; Schröder, D.; Koch, W.; Schwarz, H. *Chem. Phys. Lett.* **1995**, *236*, 194. (i) Böhme, M.; Wagener, T.; Frenking, G. *J. Organomet. Chem.* **1996**, *520*, 31. (j) Hoyau, S.; Ohanessian, G. *Chem. Phys. Lett.* **1997**, *280*, 266. (k) Sievers, M. R.; Jarvis, L. M.; Armentrout, P. B. *J. Am. Chem. Soc.* **1998**, *120*, 1891. (l) Bera, J. B.; Samuelson, A. G. *Organometallics* **1998**, *17*, 4136. (m) Schröder, D.; Schwarz, H.; Hrusák, J.; Pyykkö, P. *Inorg. Chem.* **1998**, *37*, 624. (n) Ma, N. L. *Chem. Phys. Lett.* **1998**, *297*, 230. (o) Kovács, A.; Frenking, G. *Organometallics* **1999**, *18*, 887. (p) Schröder, D.; Wesendrup, R.; Hertwig, R. H.; Dargel, T. K.; Grauel, H. Koch, W.; Bender, B. R.; Schwarz, H. *Organometallics* **2000**, *19*, 2608. (q) Boutreau, L.; Leon, E.; Luna, A.; Toulhoat, P.; Tortajada, J. *Chem. Phys. Lett.* **2001**, *338*, 74. (r) Kaneti, J.; de Smet, L. C. P. M.; Boom, R.; Zuilhof, H.; Sudholter, E. J. R. *J. Phys. Chem. A* **2002**, *106*, 11197. (s) Kim, D.; Hu, S.; Tarakeshwar, P.; Kim, K. S.; Lisy, J. M. *J. Phys. Chem. A* **2003**, *107*, 1228.
(15) Ziegler, T.; Rauk, A. *Inorg. Chem.* **1979**, *18*, 1558.
(16) Hertwig, R. H.; Koch, W.; Schröder, D.; Schwarz, H.; Hrusák, J.; Schwerdtfeger, P. *J. Phys. Chem.* **1996**, *100*, 12253.
(17) Becke, A. D. *Phys. Rev. A* **1988**, *38*, 3098.
(18) Lee, C.; Yang, W.; Parr, R. G. *Phys. Rev. B* **1988**, *37*, 785.
(19) (a) Van Lenthe, E.; Van Leeuwen, R.; Baerends, E. J.; Snijders, J. G. *Int. J. Quantum Chem.* **1996**, *57*, 281. (b) Van Lenthe, E.; Ehlers, A. E.; Baerends, E. J. *J. Chem. Phys.* **1999**, *110*, 8943, and references therein.
(20) (a) Fonseca Guerra, C.; Snijders, J. G.; Te Velde, G.; Baerends, E. J. *Theor. Chem. Acc.* **1998**, *99*, 391. (b) Te Velde, G.; Bickelhaupt, F. M.; Baerends, E. J.; Fonseca Guerra, C.; Van Gisbergen, S. J. A.; Snijders, J. G.; Ziegler, T. *J. Comput. Chem.* **2001**, *22*, 931.
(21) Dolg, M.; Stoll, H.; Preuss, H.; R. M. Pitzer, R. M. *J. Phys. Chem.* **1993**, *97*, 5852.
(22) $Ag(P_4)_2^+$ was first reported to be D_{2h}-symmetric in the solid state (ref 1). This result was surprising in light of recent quantum-chemical calculations (ref 7), which indicated that D_{2d} and D_2 conformers have the same energy. Very recent experiments confirmed the calculations. A new D_2 crystal structure with an dehedral angle of 44° has been obtained, indicating that the orientation of the two $Ag(P_2)$ planes strongly depends on the counterions (Krossing, I., unpublished results). Hypothetical $M(\eta^1\text{-}P_4)_2^+$ and $M(\eta^3\text{-}P_4)_2^+$ haptomers are predicted to be less stable (ref 5).
(23) (a) Pyykkö, P. *Chem. Rev.* **1988**, *88*, 563. (b) Almlöf, J.; Gropen, O. In *Reviews in Computational Chemistry*; Lipkowitz, K. B., Boyd, D. B., Eds.; VCH: New York, 1996; Vol. 8, p 203. (c) Balasubramanian, K. *Relativistic Effects in Chemistry*; Wiley: New York, 1997. (d) Frenking, G., Ed. *J. Comput. Chem.* **2002**, 23 (8), 759−860. Special issue: *Relativistic Methods in Quantum Chemistry*. (e) Schwerdtfeger, P., Ed. *Relativistic Electronic Structure Theory*; Elsevier: Amsterdam, 2002. (f) Pyykkö, P. *Angew. Chem., Int. Ed.* **2002**, *41*, 3573, and references therein.

Table 1. Calculated Bond Distances (in Å) in P_4 and $M(P_4)_2^+$ (D_{2h}) with M = Cu, Ag, Au

	P_4	Cu				Ag				Au			
level of theory	P−P	M−P1	P1−P2	P1−P3	P3−P4	M−P1	P1−P2	P1−P3	P3−P4	M−P1	P1−P2	P1−P3	P3−P4
BLYP/IV′ NR	2.217	2.371	2.382	2.207	2.249	2.657	2.365	2.204	2.250	2.743	2.367	2.204	2.251
BLYP/IV′ R	2.218	2.349	2.387	2.208	2.250	2.567	2.390	2.206	2.250	2.503	2.446	2.210	2.253
B3PW91/XXL	2.197	2.361	2.342	2.181	2.223	2.569	2.343	2.179	2.224	2.492	2.399	2.182	2.227

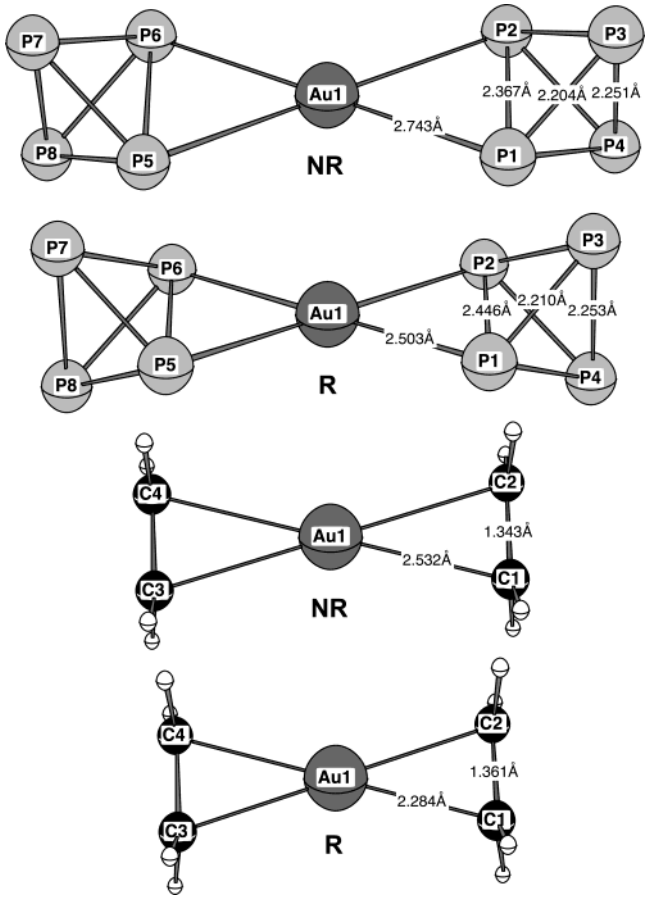

Figure 2. Structures of $Au(P_4)_2^+$ and $Au(C_2H_4)_2^+$ (D_{2h} symmetry) predicted by nonrelativistic (NR) and relativistic (R) density functional calculations at the BLYP level.

Table 2. Calculated Bond Distances (in Å) in C_2H_4 and $M(C_2H_4)_2^+$ (D_{2h}) with M = Cu, Ag, Au

	C_2H_4	Cu		Ag		Au	
level of theory	C−C	M−C	C−C	M−C	C−C	M−C	C−C
BLYP/IV′ NR	1.319	2.154	1.350	2.447	1.342	2.532	1.343
BLYP/IV′ R	1.319	2.130	1.351	2.362	1.347	2.284	1.361
B3PW91/XXL	1.327	2.130	1.356	2.351	1.354	2.270	1.368

Table 3. Calculated Stabilization Energies, $M^+ + 2\ P_4 \rightarrow M(P_4)_2^+$ (M = Cu, Ag, Au, in kcal/mol)

level of theory	Cu	Ag	Au
BLYP/IV′ NR	−110.7	−68.7	−63.8
BLYP/IV′ R	−119.8	−85.4	−135.4
B3PW91/XXL	−105.2	−77.2	−123.5

plexes. This is shown in Table 2. The metal−C bonds are shortened and the C−C bond in each ethylene ligand is elongated, compared to the nonrelativistic bond lengths.

The calculated coordination energies (reaction energies of $M^+ + 2\ L \rightarrow ML_2^+$) are given in Tables 3 and 4. Comparison of DFT-calculated energies with experimental values available for ethylene complexes shows good agreement, as discussed earlier.[5,7,16] Relativistic

Table 4. Calculated Stabilization Energies, $M^+ + 2\ C_2H_4 \rightarrow M(C_2H_4)_2^+$ (M = Cu, Ag, Au, in kcal/mol)

level of theory	Cu	Ag	Au
BLYP/IV′ NR	−95.7	−59.9	−55.7
BLYP/IV′ R	−103.3	−73.0	−114.4
B3PW91/XXL	−96.4	−71.0	−112.1

effects stabilize the metal−ligand bonds concomitantly with the metal−P and metal−C bond contraction.[23] While the silver cations with P_4 ligands were denoted "superweak complexes",[5,24] we predict relativistic coordination energies ΔE of −120, −85, and −135 kcal/mol with M = Cu, Ag, and Au, respectively (Table 3). Hence, the copper and gold congeners are significantly more stable than the experimentally known $Ag(P_4)_2^+$ cation and should be interesting targets for synthesis. The bonds to the ethylene ligands are weaker than those to the phosphorus ligands by 16, 12, and 21 kcal/mol with M = Cu, Ag, and Au, respectively, but show the same trend in stability within the group 11 triad (Table 4).

Importance of Metal (n−1)d, ns, and np Orbitals

We now analyze the nature of the metal−ligand bond in the ML_2^+ complexes by partitioning the interaction energy ΔE_{int} between M^+ and $(L)_2$ into three contributions: repulsion between metal and ligands due to the Pauli principle ΔE_{Pauli}, electrostatics ΔE_{elst}, and stabilizing orbital interactions ΔE_{orb} ($\Delta E_{int} = \Delta E_{elst} + \Delta E_{Pauli} + \Delta E_{orb}$). In particular, we will use the high symmetry (D_{2h}) of the ML_2^+ species to reveal the energy contributions from the involvement of metal (n−1)d, ns, and np orbitals. The strength of the analysis, which was pioneered by Morokuma and by Ziegler and Rauk,[8] is that chemical intuition is readily translated to a profound description of the chemical bond.

To explore the interplay between relativistic effects and geometric changes, we have investigated the gold(I) complexes in two steps (Table 5). *First*, relativistic effects are switched on, but the nonrelativistic geometry is maintained. This corresponds to the R//NR entries in Table 5. *Second*, the changes in the energy contributions upon geometrical relaxation are considered (entry R in Table 5). The calculations indicate that relativistic corrections to the contributions from Pauli repulsion (ΔE_{Pauli}) and electrostatics (ΔE_{elst}) predicted using the nonrelativistic geometries of $Au(P_4)_2^+$ are nearly equal, whereas the orbital interactions show a strong stabilization. Structural changes then lead to a large increase of electrostatics and a noticeable increase of the stabilizing orbital interactions. The concomitant increase of Pauli repulsion, however, results in a small net stabilization of the metal−P_4 bonds due to geometric relaxation by only 10 kcal/mol. Hence, the results presented

(24) Loss of translational and rotational entropy of the formally trimolecular reaction corrects the free energies by approximately 15 kcal/mol at 298 K. For instance, the entropical change ΔS of the reaction $Ag^+ + 2\ P_4 \rightarrow Ag(P_4)_2^+$ is calculated to be $\Delta S = -50.9$ cal/mol K.

Downloaded by NAT LIB UKRAINE on July 5, 2009
Published on April 15, 2004 on http://pubs.acs.org | doi: 10.1021/om034246z

Table 5. Energy Decomposition of the M−P_4 Bonds in $M(P_4)_2^+$ (D_{2h}) at the BLYP/IV′ Level (energies in kcal/mol[a])

contribution		Cu		Ag		Au		
		NR	R	NR	R	NR	R	R//NR
ΔE_{str}		8.0	8.5	6.6	8.4	6.8	13.1	6.7
ΔE_{Pauli}		147.7	158.4	110.1	145.8	114.7	246.1	106.0
ΔE_{elst}		−134.4	−144.9	−94.7	−125.3	−97.1	−213.1	−99.2
ΔE_{orb}		−132.1	−141.9	−90.7	−114.3	−88.5	−181.5	−137.4
$\Delta E_{orb}(\Gamma_i)$	**a_{1g} (s, d_{x^2-y2}, d_{z^2})**	**−56.7**	**−61.9**	**−43.9**	**−56.8**	**−46.5**	**−100.2**	**−90.2**
	b_{1u} (p_z)	**−20.7**	**−21.5**	**−15.5**	**−17.6**	**−13.7**	**−22.1**	**−17.0**
	b_{2g} (d_{xz})	**−21.2**	**−23.2**	**−9.9**	**−13.6**	**−8.9**	**−23.4**	**−10.0**
	b_{3u} (p_x)	**−17.0**	**−17.7**	**−11.0**	**−13.1**	**−9.7**	**−17.4**	**−10.3**
	b_{2u} (p_y)	**−6.5**	**−6.9**	**−4.0**	**−4.9**	**−3.5**	**−6.6**	**−3.4**
	b_{3g} (d_{yz})	**−5.6**	**−5.9**	**−3.6**	**−4.5**	**−3.4**	**−6.4**	**−3.7**
	b_{1g} (d_{xy})	**−3.0**	**−3.2**	**−1.9**	**−2.5**	**−1.8**	**−3.8**	**−1.9**
	a_{1u} (−)	**−1.5**	**−1.5**	**−1.1**	**−1.3**	**−1.0**	**−1.6**	**−0.9**
$\Delta E_{int} = \Delta E_{Pauli} + \Delta E_{elst} + \Delta E_{orb}$		−118.7	−128.3	−75.3	−93.8	−70.6	−148.5	−130.5
$\Delta E = \Delta E_{str} + \Delta E_{int}$		−110.7	−119.8	−68.7	−85.4	−63.8	−135.4	−123.8

[a] Bold: Contributions of the irreducible representations Γ_i to the stabilizing orbital-interaction energy ΔE_{orb}: Γ_i, metal orbitals involved (in parentheses), and energy ΔE_{orb} (Γ_i) in kcal/mol. The R//NR entry refers to relativistic calculations using nonrelativistic structures.

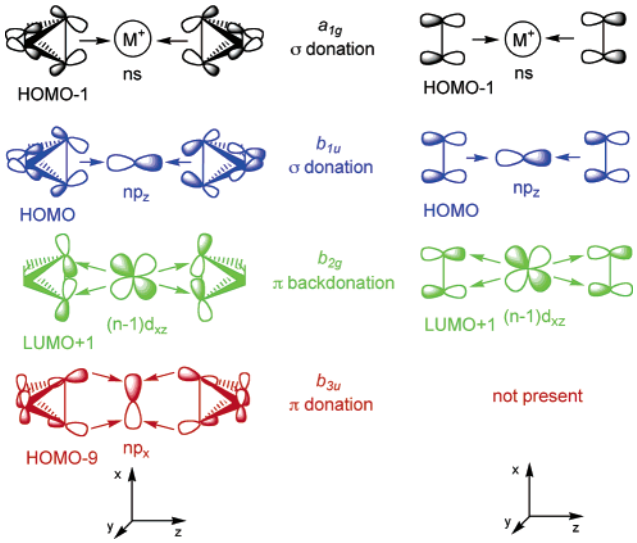

Figure 3. Interactions of symmetry orbitals in $M(P_4)_2^+$ and $M(C_2H_4)_2^+$. The b_{3u} contribution (red) is essentially absent in the ethylene complex.

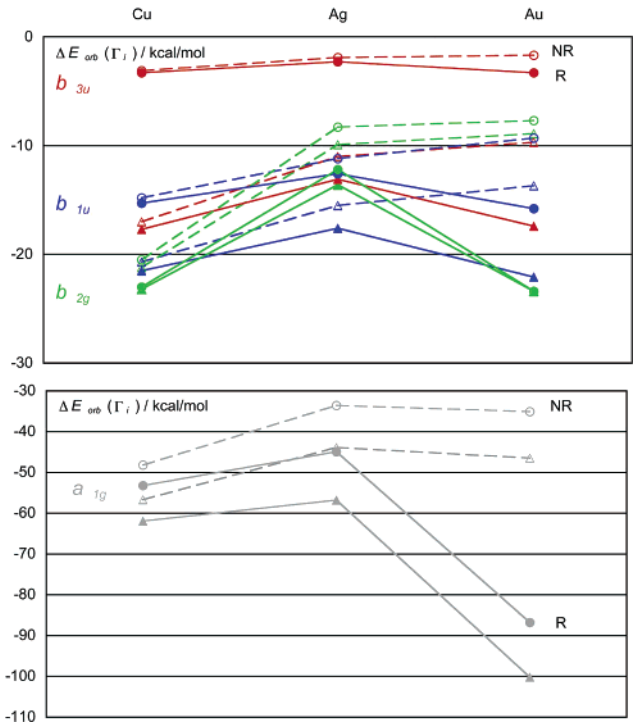

Figure 4. Contributions from symmetry orbitals to the stabilizing orbital interactions (in kcal/mol) in $M(P_4)_2^+$ (triangles) and $M(C_2H_4)_2^+$ (balls). Full symbols correspond to relativistic calculations (R); empty symbols correspond to nonrelativistic calculations (NR).

in Table 5 warrant a conclusive comparison of the orbital interactions at the nonrelativistic and relativistic levels.

The decomposition of the orbital interactions into symmetry orbitals is of particular interest, because the contributions involving the metal $(n-1)$d, ns, and np orbitals to the orbital interaction energy become accessible. Table 5 presents the results of the analysis of $M(P_4)_2^+$ (M = Cu, Ag, Au). The most important symmetry orbital interactions are displayed in Figure 3, and their energy contributions are plotted in Figure 4. We focus in the discussion first on the *tetrahedro*-phosphorus complexes of gold(I) represented by triangles in Figure 4. The empty symbols in Figure 4 correspond to nonrelativistic calculations, and the filled symbols correspond to relativistic calculations. The relativistic calculations show that σ donation from P_4 into the metal 6s orbital (a_{1g}, gray)[25] causes only half of the stabilizing orbital interactions in the gold(I) complexes, followed by an unexpectedly large amount of $5d^{10}$-closed-shell π back-donation into σ^*(P−P) orbitals (b_{2g}, green), by σ donation from P_4 into the metal $6p_z$ orbital (b_{1u}, blue), and by π donation from from P_4 into the metal $6p_x$ orbital (b_{3u}, red).

The results given in Figure 4 reveal a relativistic increase of the interactions within each orbital symmetry, but to a different extent. Electron back-donation from the metal $5d_{xz}$ orbital (b_{2g}, green) shows the largest relative energy gain due to relativistic effects (62%), followed by donation into the vacant metal 6s orbital (a_{1g}, gray, 54%) and by donation into the vacant metal 6p orbitals (b_{3u}, red, 44% and b_{1u}, blue, 38%). To elucidate this finding, we have calculated the frontier-orbital energies of the metal cations (Figure 5). Today it is known[23] that the speed of electrons in the 1s and

(25) Note that the $(n-1)d_{z^2}$ and $(n-1)d_{x^2-y^2}$ orbitals also have a_{1g} orbital symmetry. These orbitals are occupied and a respective symmetry-adapted linear combination of ligand orbitals is not available.

Downloaded by NAT LIB UKRAINE on July 5, 2009
Published on April 15, 2004 on http://pubs.acs.org | doi: 10.1021/om034246z

Table 6. Overlap Integrals between Ligand and Metal Orbitals in $M(P_4)_2^+$

		Cu		Ag		Au		
Γ_i	overlap	NR	R	NR	R	NR	R	R//NR
a_{1g}	$\langle$HOMO−1$\|ns\rangle$	0.414	0.418	0.366	0.389	0.350	0.413	0.348
b_{1u}	$\langle$HOMO$\|np_z\rangle$	0.378	0.375	0.374	0.388	0.387	0.433	0.419
b_{2g}	$\langle$LUMO+1$\|(n-1)d_{xz}\rangle$	0.109	0.111	0.107	0.120	0.112	0.156	0.115
b_{3u}	$\langle$HOMO−9$\|np_x\rangle$	0.485	0.489	0.407	0.427	0.395	0.432	0.345

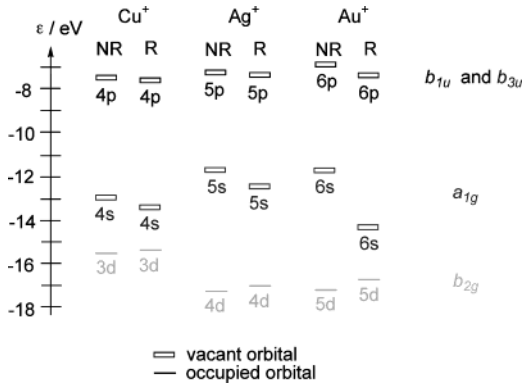

Figure 5. Calculated frontier-orbital energies of the metal cations (in eV). For frontier-orbital energies of the ligands, see Supporting Information.

2s orbitals close to the nucleus reaches the magnitude of the speed of light, leading to a contraction of these orbitals. As a secondary effect, arising from the fact that the outer s electrons have appreciable density near the nucleus and are shielded more poorly by valence and outer core d and f shells, the outer s orbitals such as 6s contract as well and are thus stabilized. A tertiary effect is the stronger shielding of the nuclear charge by the electrons in contracted s orbitals. The 5d orbitals experience a smaller nuclear charge than they would in the absence of relativity. Hence, they expand and their energy levels rise. 6p orbitals become slightly more stable (Figure 5).

When evaluating relativistic effects on the stabilizing orbital interactions, one has to consider whether the respective orbitals are donor or acceptor orbitals. Figure 5 shows that the lowering of the 6s-orbital-energy level of gold(I) is particularly strong, resulting in its greater electron-acceptor ability and therefore in a large energy increase of the interactions of this orbital (a_{1g}, gray, Figures 3 and 4). It is interesting to note that the energy level of the $5d_{xz}$ donor orbital rises only slightly, but the corresponding interaction shows the largest relative increase due to relativistic effects. This remarkable result points to the importance of the overlap between metal and ligand orbitals (Table 6), in addition to the energy levels of the orbitals. While all overlap integrals listed in Table 6 increase due to relativity, the largest relative change in the overlap integrals is indeed observed for $\langle(n-1)d_{xz}|$LUMO+1$\rangle$ of b_{2g} orbital symmetry. Note that the d orbitals expand, increasing their overlap with the ligands.

In the case of the b_{2g} and b_{3u} interactions, we observe a considerable effect of a geometric change on the energy (see entries R//NR and R in Table 5). This is evident from a comparison of the relativistic calculations of the energy contributions and overlap integrals using the nonrelativistic and relativistic geometries of $Au(P_4)_2^+$ (R//NR and R entries in Table 5). Note that both b_{2g} (green) and b_{3u} (red) are π interactions (Figure 3). The sensitivity of π interactions to the molecular structure may be rationalized by the fact that π interactions require shorter interatomic distances than do σ interactions.[26]

A comparison of the bond-energy contributions in the $Au(C_2H_4)_2^+$ complex and its η^2-P_4 counterpart indicates a striking similarity. An exception is the missing contribution from ethylene orbitals into the metal np_x orbital (b_{3u}, red). A b_{3u} linear combination of occupied ethylene orbitals is not available (Figure 3), resulting in a very small b_{3u} component (red circles in Figure 4). Analyzing the orbitals reveals that the *donor* orbitals of $(P_4)_2$ (i.e., those involved in a_{1g}, b_{1u}, and b_{3u}) mainly—but not only—consist of p orbitals of the *proximal* phosphorus atoms (P1, P2, P5, P6). They also contain p orbitals of the *distal* phosphorus atoms (P3, P4, P7, P8).[27] In contrast, the b_{2g} *acceptor* orbital of $(P_4)_2$ corresponds to the σ^* bonds between the proximal P atoms. This effect leads to the interesting phenomenon that the calculated atomic charges at the distal P atoms in $Au(P_4)_2^+$ are more positive than those at the proximal P.[28]

Comparison of CuL_2^+, AgL_2^+, and AuL_2^+

We now compare the bonding in the experimentally known $Ag(P_4)_2^+$ cation[1] to that in the copper and gold analogues. The calculations reveal a nearly quantitative match of the bond-energy contributions in the nonrelativistic silver and gold complexes, indicating that the differences between $Ag(P_4)_2^+$ and the heavier congener can be attributed to relativity (Figure 4). Even in the lighter copper and silver species, $Cu(P_4)_2^+$ and $Ag(P_4)_2^+$, the relativistic corrections to the bond energies are found to be as large as 9 and 17 kcal/mol, respectively (Table 3).

The copper-phosphorus complex is predicted to be much more stable than the parent silver cation (Table 5). The analysis of $Cu(P_4)_2^+$ reveals that the b_{2g} interactions involving the $3d_{xz}$ orbital of Cu^+ are particularly large, much larger than the corresponding interaction in $Ag(P_4)_2^+$. This is a remarkable result. 3d orbitals are the first orbitals of this type, and inner d orbitals to which the 3d orbitals must be orthogonal are not present. Hence, 3d orbitals penetrate deeply into the core region. The smaller size of the 3d orbitals led to the suggestion that first-row transition metals form weaker bonds to ligands because of the smaller overlap of ligand orbitals with the metal 3d orbitals compared to that with the 4d orbitals of second-row transition metals. This suggestion became a central hypothesis of a textbook.[29] Our analysis of highly symmetric com-

(26) For example, see: Deubel, D. V.; Frenking, G.; Senn, H. M.; Sundermeyer, J. *Chem. Commun.* **2000**, 2469.
(27) See Supporting Information for details.
(28) Calculated Hirshfeld charges (Hirshfeld, E. L. *Theor. Chim. Acta* **1977**, *44*, 129): In $Au(P_4)_2^+$, Au 0.20, proximal P 0.08, distal P 0.12. In $Au(C_2H_4)_2^+$, Au 0.41, each C_2H_4 0.29.

Downloaded by NAT LIB UKRAINE on July 5, 2009
Published on April 15, 2004 on http://pubs.acs.org | doi: 10.1021/om034246z

Downloaded by NAT LIB UKRAINE on July 5, 2009
Published on April 15, 2004 on http://pubs.acs.org | doi: 10.1021/om034246z

plexes provides a critical assessment of the hypothesis in the case of late metal complexes. We have calculated the overlap integrals $\langle((n-1)d_{xz}|LUMO+1)\rangle$ between the metal d_{xz} orbital and the corresponding ligand orbitals (b_{2g}); the results are collected in Table 6. In contrast to the textbook hypothesis, we demonstrate that these overlap integrals in the copper and silver compounds are essentially equal. This may be attributed partly to the larger P−Cu−P angle (61°) in comparison with the P−Ag−P angle (55°), arising from the fact that the Cu−ligand distances are shorter than the Ag−ligand distances. A large P−metal−P angle likely favors the overlap of the corresponding σ^*(P−P) orbitals with the 90° lobes of the metal d_{xz} orbital. The orbital-energy levels displayed in Figure 5 show that the 3d orbitals of Cu^+ are significantly higher in energy than the 4d orbitals of Ag^+. Because there are no nodes in the 3d shell, the electron−electron repulsion in this shell of Cu^+ becomes unusually strong and increases the orbital energy compared to that of the 4d shell of Ag^+. Therefore, copper(I) becomes a better back donor than silver(I), as reflected by the strength of the b_{2g} interactions. Note that earlier transition metals with a partial occupation of 3d orbitals may form weaker bonds to ligands than do their 4d congeners, because (vacant) 3d orbitals, which are higher in energy than the 4d orbitals, are weaker acceptor orbitals. However, these weaker bonds are unlikely caused by smaller overlap integrals.

Preliminary calculations show that the periodic trends can be extrapolated from $Ag(C_2H_4)_2^+$ and $Au(C_2H_4)_2^+$ to the ethylene complexes of the transactinide cation unununium(I) (Uuu, element 111) in an analogue $6d^{10}7s^0$ ($^1S_0$) state. However, the large relativistic stabilization of the 7s orbital of Uuu^+ leads to a different ground state. The ground state of Uuu^+ is $6d^87s^2$ ($^3D_4$), which is lower in energy than the $6d^{10}7s^0$ ($^1S_0$) state by 4.73 eV (109.0 kcal/mol). This was shown by four-component relativistic coupled cluster calculations of Uuu^+ ions.[30] The structural and electronic properties of superheavy element organometallics probably do not fit the scheme derived here for the complexes of coinage-metal cations. Extrapolating chemically relevant trends such as orbital-energy levels may lead to a different chemistry.

Conclusions

Density functional calculations have been carried out to predict and rationalize the factors governing periodic trends in the involvement of $(n-1)$d, ns, and np orbitals in metal−ligand interactions. Organometallics and *tetrahedro* phosphorus complexes, $M(\eta^2\text{-}P_4)_2^+$ and $M(C_2H_4)_2^+$, of the coinage metals, M = Cu, Ag, and Au, have been selected due to a historical and current interest in these compounds. The D_{2h} point group of these molecules allows for an analysis of symmetry orbitals guided by chemical intuition.

The metal−ligand bonds in $Au(\eta^2\text{-}P_4)_2^+$ are stronger than those in $Ag(\eta^2\text{-}P_4)_2^+$, which is attributed to relativistic effects. The bonding components of nonrelativistic $Au(\eta^2\text{-}P_4)_2^+$ and $Ag(\eta^2\text{-}P_4)_2^+$ show an almost quantitative agreement. Relativistic effects increase the relative contributions to the orbital-interaction energy in the following order: electron donation (from ligands) into metal np acceptor orbitals < donation into metal ns acceptor orbitals < back-donation from $(n-1)$d orbitals. This result can be understood by considering (i) the occupation of the metal orbitals, i.e., whether they are involved in donation or back-donation, (ii) the change in their energy due to relativity, e.g., 6s orbitals are strongly stabilized and 5d orbitals are destabilized, and (iii) the change in their size, e.g., the relativistic expansion of 5d orbitals increases their overlap with ligand orbitals. The relativistic stabilization of the ns orbitals and the destabilization of the $(n-1)$d orbitals continues to the group 11 transactinide cation unununium(I). However, this extrapolation of trends leads to a ground state of Uuu^+ that is different from $6d^{10}7s^0$, implying an entirely different chemistry of the superheavy element cation.

The metal−ligand bonds in $Cu(\eta^2\text{-}P_4)_2^+$ are also stronger than those in $Ag(\eta^2\text{-}P_4)_2^+$. This result is partly attributed to the increase in the interactions involving 3d orbitals. Following textbook suggestions, one would have anticipated that the bond energies in 3d element complexes are smaller than those in 4d element complexes due to a smaller overlap between 3d and ligand orbitals. In contrast, our quantum-chemical calculations reveal similar overlap integrals in the case of 3d and 4d metals. A significant increase of the 3d orbital energy level in Cu^+ (relative to that of 4d in Ag^+) enhances electron back-donation from the *occupied* 3d orbital of copper(I) to the ligands. This higher energy level of 3d orbitals relative to 4d is likely the reason for smaller bond energies of earlier first-row transition metal complexes, when 3d orbitals are *vacant* and become weaker acceptor orbitals.

Our analysis demonstrates a similarity of ethylene and white phosphorus as η^2 ligands consistently throughout the coinage-metal triad. The main differences are an additional symmetry-adapted linear combination of phosphorus orbitals interacting with the metal and the involvement of the distal phosphorus atoms in electron donation to the metal. In future studies, we intend to analyze metal complexes with several organic and inorganic ligands, aiming at a quantitative interpretation of isolobal analogy based on symmetry orbitals and their energy contributions.

Computational Methods

General Procedure. Geometry optimizations and energy calculations were performed at the gradient-corrected density functional theory (DFT) level using Becke's exchange functional[17] and Lee, Yang, and Parr's[18] correlation functional (BLYP) as implemented in the Amsterdam Density Functional 2000 program (ADF). Uncontracted Slater-type orbitals (STOs) were used as basis functions.[31] The valence basis functions at Cu, Ag, and Au have triple-ζ quality, augmented with a set of p functions. The valence basis set at P has triple-ζ quality, augmented with a set of d and f functions. The valence basis set at the other atoms has triple-ζ quality, augmented with a set of d functions. The $(1s)^2$ core electrons of C, the $(1s2s2p)^{10}$ core electrons of P, the $(1s2sp3spd)^{28}$ core electrons of Ag, and the $(1s2sp3spd4spd)^{46}$ core electrons of Au were treated within the frozen-core approximation.[32] This basis-set combination is

(29) Gerloch, M.; Constable, E. C. *Transition Metal Chemistry*; VCH: Weinheim, 1994.

(30) Eliav, E.; Kaldor, U.; Schwerdtfeger, P.; Hess, B. A.; Ishikawa, Y. *Phys. Rev. Lett.* **1994**, *73*, 3203. 2469.

(31) Snijders, J. G.; Baerends, E. J.; Vernooijs, P. *At. Data Nucl. Tables* **1982**, *26*, 483.

Downloaded by NAT LIB UKRAINE on July 5, 2009
Published on April 15, 2004 on http://pubs.acs.org | doi: 10.1021/om034246z

denoted IV′. Geometry optimizations and energy calculations were also carried out using Becke's DFT−Hartree−Fock hybrid method,[33] which includes Perdew and Wang's correlation functional[34] (B3PW91) as implemented in Gaussian 98 (G98).[35] An energy-consistent scalar-relativistic small-core effective core potential (ECP)[21] with the corresponding basis set fully decontracted and augmented with a set of f functions[36] was employed for the metals, while the basis sets 6-311+(3df) and 6-311+(2d,p) were used at phosphorus and at the other atoms, respectively. This basis-set combination is denoted XXL. The stationary points calculated at B3PW91/XXL were characterized by zero imaginary frequencies. Additional calculations at various levels of theory using the ADF and G98 programs were reported in the Supporting Information of ref 7.

Consideration of Relativistic Effects. Evaluating the time-independent Dirac equation:[37]

$$(c\alpha p + \beta mc^2 + V)\psi = E\psi \tag{1}$$

in 2 × 2-block-diagonal form, gives the relation between the small component ψ_S and the large component ψ_L of the Dirac spinor ψ as the branching point of the first-order method (FO)[38] and the zeroth-order regular approximation (ZORA):[19]

$$\psi_S = (2mc^2 + E - V)^{-1} c\sigma p \psi_L = \lambda\, c\sigma p \psi_L \tag{2}$$

Factoring out $(2mc^2)^{-1}$ and expanding in first-order leads to the FO approach:

$$\lambda_{FO} = (2mc^2)^{-1}\left(1 + \frac{E-V}{2mc^2}\right)^{-1} \approx (2mc^2)^{-1}\left(1 - \frac{E-V}{2mc^2}\right) \tag{3}$$

and to the Pauli equation:

$$\left(\frac{p^2}{2m} + V + \frac{Zs(r \times p)}{2m^2c^2r^3} - \frac{p^4}{8m^3c^2} + \frac{Z\pi\delta(r)}{2m^2c^2}\right)\psi_L = E\psi_L \tag{4}$$

with the Schrödinger Hamiltonian ($p^2/2m + V$) and the spin−orbit, mass-velocity, and Darwin corrections. The latter two terms are denoted scalar-relativistic corrections. The first-order results can significantly be improved by a quasi-relativistic approach (QR),[39] where the energy corrections consider relativistic changes in electron density. However, in the case of the singular Coulomb potential, the expansion in $(E - V)/2mc^2$ diverges near the nucleus.[19] This can be circumvented by using the zeroth-order regular approximation (ZORA),[19] which is obtained from eq 2 by factoring out $(2mc^2 - V)^{-1}$ and expanding in zeroth order:

$$\lambda_{ZORA} = (2mc^2 - V)^{-1}\left(1 + \frac{E}{2mc^2 - V}\right)^{-1} \approx (2mc^2 - V)^{-1} \tag{5}$$

In the present work, the scalar-relativistic ZORA method was utilized and the results were compared to those from nonrelativistic calculations. Spin−orbit effects were considered by ZORA energy calculations of the gold(I) complexes using the scalar-relativistic geometries, showing that these effects are very small (<2 kcal/mol). Unless otherwise mentioned, "relativistic effects" refer to the differences between the NR and scalar-relativistic ZORA results calculated at the BLYP/IV′ level using the ADF program.

Bonding Analysis. The decomposition of the metal−ligand bond energies was examined using an energy-decomposition scheme.[8,9,40] The ML_2^+ molecules were divided into the M^+ and L_2 fragments. The stabilization energy ΔE is partitioned into the two contributions strain energy, ΔE_{str}, and interaction energy, ΔE_{int}:

$$\Delta E = \Delta E_{str} + \Delta E_{int} \tag{6}$$

The strain energy ΔE_{str} is the difference between the energy of the isolated fragments in the geometry of ML_2^+ and their energy in the equilibrium geometry of M^+ and L_2. ΔE_{int} represents the energy of interaction between the fragments in the complex geometry and can in turn be partitioned into three components:

$$\Delta E_{int} = \Delta E_{elst} + \Delta E_{Pauli} + \Delta E_{orb} \tag{7}$$

ΔE_{elst} gives the electrostatic interaction energy between the fragments, which is calculated with a frozen electron-density distribution in the TS geometry of ML_2^+. ΔE_{Pauli} is the repulsive interaction energy between the fragments that is caused by the fact that two electrons with the same spin cannot occupy the same region in space. ΔE_{Pauli} is calculated by enforcing the Kohn−Sham determinant which is the result of the two superimposing M^+ and L_2 fragments to obey the Pauli principle through antisymmetrization and renormalization. Finally, the orbital-interaction term ΔE_{orb} is calculated with the Kohn−Sham orbitals relaxing to their optimal form. This scheme may also be applied to transition states.[41] ΔE_{orb} can be partitioned into the contributions from the irreducible representations Γ_i.

Acknowledgment. D.V.D. and I.K. thank the Fonds der Chemischen Industrie and the Federal Ministry of Education and Research, Germany, for Liebig Fellowships.

Supporting Information Available: Calculated structures and energies of conformers and analysis of frontier orbitals of metal ions and ligands. This material is available free of charge via the Internet at http://pubs.acs.org.

OM034246Z

(32) Baerends, E. J.; Ellis, D. E.; Ros, P. *Chem. Phys.* **1973**, *2*, 41.
(33) Becke, A. D. *J. Chem. Phys.* **1993**, *98*, 5648.
(34) Perdew, J. P.; Wang, Y. *Phys. Rev.* **1992**, *B45*, 13244.
(35) Frisch, M. J.; Trucks, G. W.; Schlegel, H. B.; Scuseria, G. E.; Robb, M. A.; Cheeseman, J. R.; Zakrzewski, V. G.; Montgomery, J. A.; Stratmann, R. E.; Burant, J. C.; Dapprich. S.; Milliam, J. M.; Daniels, A. D.; Kudin, K. N.; Strain, M. C.; Farkas, O.; Tomasi, J.; Barone, V.; Cossi, M.; Cammi, R.; Mennucci, B.; Pomelli, C.; Adamo, C.; Clifford, S.; Ochterski, J.; Petersson, G. A.; Ayala, P. Y.; Cui, Q.; Morokuma, K.; Malick, D. K.; Rabuck, A. D.; Raghavachari, K.; Foresman, J. B.; Cioslowski, J.; Ortiz, J. V.; Stefanov, B. B.; Liu, G.; Liashenko, A.; Piskorz, P.; Komaromi, I.; Gomberts, R.; Martin, R. L.; Fox, D. J.; Keith, T. A.; Al-Laham, M. A.; Peng, C. Y.; Nanayakkara, A.; Gonzalez, C.; Challacombe, M.; Gill, P. M. W.; Johnson, B. G.; Chen, W.; Wong, M. W.; Andres, J. L.; Head-Gordon, M.; Replogle, E. S.; Pople, J. A. *Gaussian 98*; Gaussian Inc.: Pittsburgh, PA, 1998.
(36) Ehlers, A. W.; Böhme, M.; Dapprich, S.; Gobbi, A.; Höllwarth, A.; Jonas, V.; Köhler, K. F.; Stegmann, R.; Veldkamp A.; Frenking, G. *Chem. Phys. Lett.* **1993**, *208*, 111.
(37) Dirac, P. A. M. *Proc. R. Soc. London* **1928**, *117*, 610.
(38) (a) Snijders, J. G.; Baerends, E. J. *Mol. Phys.* **1979**, *36*, 1789. (b) Snijders, J. G.; Baerends, E. J.; Ros, P. *Mol. Phys.* **1979**, *38*, 1909.
(39) Ziegler, T.; Tschinke, V.; Baerends, E. J.; Snijders, J. G.; Ravenek, W. *J. Phys. Chem.* **1989**, *93*, 3050.
(40) Recent examples: (a) Diefenbach, A.; Bickelhaupt, F. M.; Frenking, G. *J. Am. Chem. Soc.* **2000**, *122*, 6449. (b) Bickelhaupt, F. M.; DeKock, R. L.; Baerends, E. J. *J. Am. Chem. Soc.* **2002**, *124*, 1500. (c) Deubel, D. V. *J. Am. Chem. Soc.* **2002**, *124*, 5834. (d) Guerra, C. F.; Bickelhaupt, F. M. *Angew. Chem., Int. Ed.* **2002**, *41*, 2012. (e) Deubel, D. V.; Ziegler, T. *Organometallics* **2002**, *21*, 1603. (f) Cases, M.; Frenking, G.; Duran, M.; Solà, M. *Organometallics* **2002**, *21*, 4182. (g) Deubel, D. V. *Organometallics* **2002**, *21*, 4303. (h) Deubel, D. V.; Ziegler, T. *Organometallics* **2002**, *21*, 4432. (i) Nemcsok, D. S.; Kovács, A.; Rayón, V. M.; Frenking, G. *Organometallics* **2002**, *21*, 5803. (j) Pandey, K. K.; Lein, M.; Frenking, G. *J. Am. Chem. Soc.* **2003**, *125*, 1660. (k) Lein, M.; Frunzke, J.; Frenking, G. *Angew. Chem., Int. Ed.* **2003**, *42*, 1303. (l) Esterhuysen, C.; Frenking, G. *Chem. Eur. J.* **2003**, *9*, 3518. (m) Massera, C.; Frenking, G. *Organometallics* **2003**, *22*, 2758. (n) Rayón, V. M.; Frenking, G. *Organometallics* **2003**, *22*, 3304. (o) Lein, M.; Frunzke, J.; Frenking, G. *Inorg. Chem.* **2003**, *42*, 2504. (p) Dietz, O.; Rayón, V. M.; Frenking, G. *Inorg. Chem.* **2003**, *42*, 4977.
(41) (a) Diefenbach, A.; Bickelhaupt, F. M. *J. Chem. Phys.* **2001**, *115*, 4030. (b) Deubel, D. V. *J. Phys. Chem. A* **2001**, *105*, 4765. (c) Deubel, D. V. *J. Phys. Chem. A* **2002**, *106*, 431. (d) Deubel, D. V. *J. Am. Chem. Soc.* **2004**, *126*, 996. (e) Deubel, D. V.; Muñiz, K. *Chem. Eur. J.* **2004**, *10*, in press.